OPEN ACCESS

University of BRISTOL

Dombovari, Z., Wilson, R. E., & Stepan, G. (2008). Estimates of the bistable region in metal cutting.

PDF-document

University of Bristol - Explore Bristol Research

General rights

Estimates of the bistable region in metal cutting

BY ZOLTAN DOMBOVARI[1,*], R. EDDIE WILSON[2]
AND GABOR STEPAN[1]

[1] *Department of Applied Mechanics, Budapest University of Technology and Economics, Budapest, H-1521, Hungary*
[2] *Department of Engineering Mathematics, University of Bristol, Bristol, BS8 1TR, United Kingdom*

The classical model of regenerative vibration is investigated with new kinds of nonlinear cutting force characteristics. The standard nonlinear characteristics are subjected to a critical review from the nonlinear dynamics viewpoint based on experimental results available in the literature. The proposed nonlinear model includes finite derivatives at zero chip thickness and has an essential inflexion point. In the case of the one degree of freedom model of orthogonal cutting, the existence of unstable self-excited vibrations is proven along the stability limits, which is strongly related to the force characteristic at its inflexion point. An analytical estimate is given for a certain area below the stability limit where stable stationary cutting and a chaotic attractor coexist. It is shown how this domain of bi-stability depends on the theoretical chip thickness. The comparison of these results to experimental observations and also to the subcritical *Hopf bifurcation* results obtained for standard nonlinear cutting force characteristics provides relevant information on the nature of the cutting force nonlinearity.

Keywords: Hopf bifurcation; bi-stable zones; metal cutting; turning; limit cycle; subcritical

1. Introduction

One of the main goals of cutting process optimization methods is to maximise the volume of the chip cut within a certain time. There are several boundaries identified in the operational space of the cutting parameters, namely, chip width, chip thickness and the cutting speed. These boundaries are related to the maximum power, maximum cutting force, feed rate, depth of cut, etc. The most difficult boundary to model is the onset of harmful relative vibrations between the tool and the work-piece. The so-called regenerative effect (where the tool interacts with its delayed displacement via the surface profile that is cut one revolution earlier) is considered to be one of the main reasons for these vibrations, which cause poor surface quality or, in extreme cases, damage the machine tool structure.

The regenerative effect for the simple orthogonal cutting model was first introduced and analysed in the middle of the 20th century (Tlusty & Spacek 1954; Tobias 1965). The central idea of this effect is that the motion of the tool depends on its past motion, in other words, a time delay occurs in the slightly damped oscillator model of the machine tool. This delay is inversely proportional to the cutting speed. The first thorough and detailed experiments on the *nonlinear* regenerative vibrations often showed small domains of attraction around stable stationary cutting (Shi & Tobias 1984). These investigations demonstrated that stable stationary cutting can be quite sensitive to external perturbations and stable, large-amplitude vibrations can appear even in those parameter domains where the stationary cutting is linearly stable.

A rigorous analytical investigation of the nature of the loss of stability of stationary cutting was performed only much later only by means of the Centre Manifold reduction and Normal Form calculations (Stepan 1997; Kalmár-Nagy *et al.* 2001).
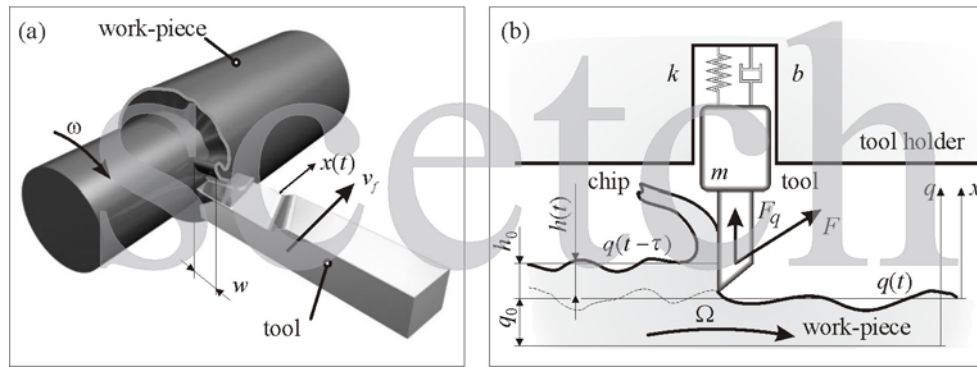
Figure 1. Panel (a) shows the arrangement of the machine tool–work-piece system in orthogonal cutting. Panel (b) illustrates a planar mechanical model.

The subcritical sense of the cutting process has been shown for several other cutting models too (Nayfeh *at al.* 1997; Kalmár-Nagy & Pratt 1999; Szalai *et al.* 2004; Campbell & Stone 2004; Wahi & Chatterjee 2005). In the substantial situation, the bifurcating local unstable orbit separates two independent attractors, namely stationary cutting and a large amplitude nonlinear oscillation that is itself stable in a dynamical systems sense. In engineering, this latter vibration is often referred to as 'instability' by owing to its harmful nature. The region where this co-existence can occur is called the region of *bi-stability*, while the terminology *unsafe zone* is used for the same idea in production technology to indicate possible chatter.

Despite the fact that large-amplitude vibrations are of little interest from a technological standpoint, the location and size of the bi-stable domain are important. This is because they define the parameter region where the cutting process is more or less sensitive to perturbations caused by, e.g., non-homogeneous work-piece material. Some of the existing software packages used for technological parameter optimisation are capable of predicting the linearly stable parameter domains for many types of cutting tools, work-pieces and machine tool configurations, but they are unable to predict those unsafe zones within the stable domain where unexpected and persistent vibrations can still occur during otherwise stable machining.

In this paper, we give a critical discussion of available nonlinear cutting force characteristics models partly from the point of view of simple geometric characteristics (e.g. derivative at zero chip thickness and the existence of an inflexion point). For the proposed nonlinear model, the subcriticality of the *Hopf bifurcation* is proven, which is related to the cutting force characteristics at a putative inflexion point. With the help of analytical and semi-analytical investigations, the location and the size of the bi-stable regions are then given. These regions are characterised as a function of the theoretical chip thickness, which is strongly related to the existence of an inflexion point in the cutting force. Experimental results (Shi & Tobias 1984; Endres & Loo 2002) in the literature confirm the validity of these conclusions in terms of direct cutting force measurements and the identification of the bi-stable region.

2. Model construction

The description of chip separation during cutting is a challenging task in both modelling and mathematical treatment. Several authors have used finite element models to try to describe accurately the coupled nonlinear physical effects near the cutting edge (Davies & Burns 2001; Stone *et al.* 2006). While these models simulate realistic cutting processes well, the structure and dependence on parameters of the consequent nonlinear vibrations remain hidden. In contrast, physical effects during cutting can be modelled more simply by means of empirical nonlinear cutting force characteristics based on the extensive measurement results of the production technology community. The large-scale geometric and elastic nonlinearities of the machine tool structure have far smaller influence on the nonlinear vibrations than those of the cutting force characteristics that exist on a small scale. In addition, the linear elasticity of the

machine tool is modelled in the direction of the essential mode only, which is related to the lowest natural frequency of the structure and supposed to be perpendicular to the cut surface.

Thus, the mechanical model used here is a simple one degree-of-freedom (DOF) damped oscillator subjected to a nonlinear cutting force F (see Figure 1). The corresponding governing equation has the form

$$\ddot{q}(t) + 2\kappa\,\omega_n\,\dot{q}(t) + \omega_n^2\,q(t) = \frac{1}{m}F_q(t),\qquad(1)$$

where ω_n and κ are the natural angular frequency and the damping ratio of the essential vibration mode described by the general coordinate q that refers to the tool position. We can express these parameters with modal mass m, stiffness k and damping factor b (see Figure 1(b)): here $\omega_n = \sqrt{k/m}$, $\kappa = b/(2m\omega_n)$, while $F_q(t)$ is the corresponding component of the resultant cutting force $F(t)$.

a) Empirical cutting force characteristics

The most popular and generally applied relation for nonlinear cutting force characteristics is the power-law

$$F_q(t) = K_q w h^\nu(t);\qquad 0 < \nu < 1,\qquad(2)$$

where w and h are the chip width and chip thickness of the orthogonal cutting, and K_q and ν are empirical parameters depending on the cutting conditions (material, tool geometry, etc.). The exponent ν may vary from 2/5 (Kalmár-Nagy & Pratt 1999) through the most popular choice 3/4 (Kienzle 1957) to 4/5 (Tlusty & Spacek 1954). The power expressions for cutting force introduced in order to enable linear optimisation tasks in the log-log space of the technological parameters (Taylor 1907).

Another approach to modelling cutting force characteristics is to fit a polynomial function to the experimental data. One of these less frequently used expressions is the cubic polynomial approximation (Shi & Tobias 1984) of the cutting force characteristics:

$$F_q(h(t)) = w(\rho_1\,h(t) + \rho_2\,h^2(t) + \rho_3\,h^3(t)).\qquad(3)$$

Clearly, here ρ_1 and ρ_3 are positive because the cutting force has positive gradient both at low and at high values of the chip thickness (see Figure 2). The potentially negative value for ρ_2 allows the existence of an inflexion point on the cutting force characteristics at

$$h_{inf} = -\frac{1}{3}\frac{\rho_2}{\rho_3}.\qquad(4)$$

From a dynamics viewpoint, there are essential differences between the two empirical interpretations (2) and (3) of the cutting force. One of these differences has a rather theoretical (or philosophical) nature. The traditional power-law characteristics have a vertical tangent at the origin (see Figure 2(a)), where the tool just touches the surface of the work-piece with zero chip thickness. This feature causes problems in the mathematical treatment of the vibrations at the loss of contact because the uniqueness and regularity of solutions no longer holds here. Apart from causing uncertainties and unpredictable errors in numerical simulations, this non-uniqueness of solutions in forward time is questionable in physical systems.
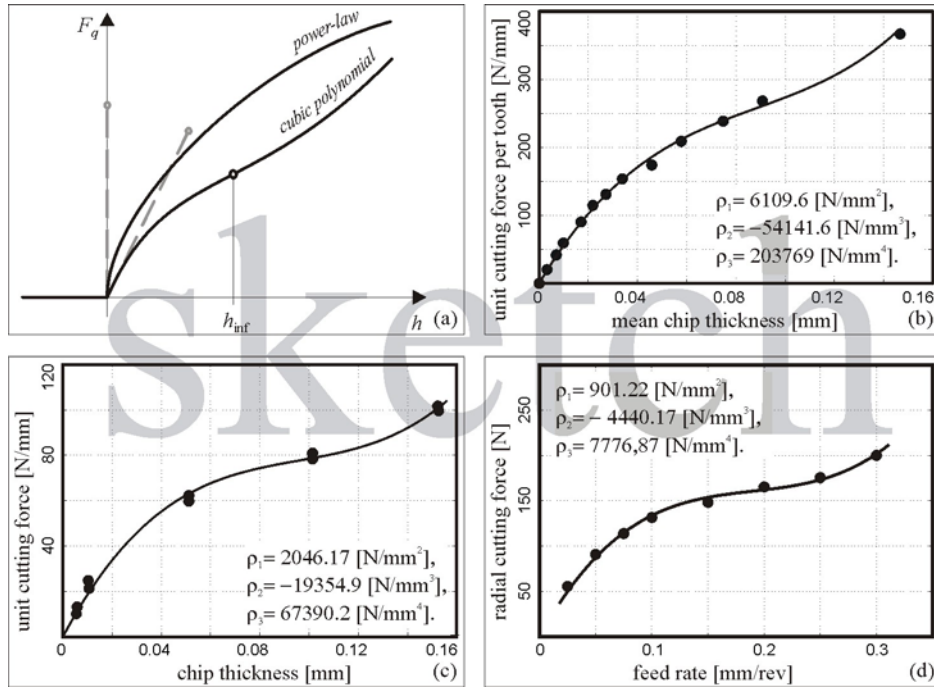
Figure 2. Panel (a) illustrates the power and the cubic forms of the empirical nonlinear cutting force characteristics. Panel (b) shows the result of *Tobias'* classical measurements (Shi & Tobias 1984) in the case of full immersion milling with a face mill with an even number of teeth. Panel (c) shows the fitted cubic cutting force characteristics measured by *Endres* in case of turning (Endres & Loo 2002). Panel (d) shows static cutting force measurements made using orthogonal cutting conditions (see, Acknowledgement).

The other important difference between the power-law (2) and the cubic polynomial force characteristics (3) is related to the possible existence of an inflexion point (see Figure 2(a)).

In the literature, there are several extensive measurement results which provide a basis for cubic polynomial approximations of the cutting force both for milling and turning. *Tobias* and *Hanna* (Shi & Tobias 1984) performed measurements based on full immersion milling with a face mill of 24 teeth. Due to the high number of cutting edges, the time periodicity of the parametric tooth-pass excitation could be averaged, and the mean cutting force characteristics with respect to the mean chip thickness were found to exhibit an inflexion point (Figure 2(b)).

Another set of experimental data measured by (Endres & Loo 2002) during valve seat turning also shows the existence of an inflexion point in the cutting force characteristics (Figure 2 (c)). However, the authors fitted an exponential function to the measured data, and hence the inflexion point could not appear in the analytical approximation and so its effect was not examined further.

The many combinations of cutting tool and work-piece material require lot of measurements using different speeds, feeds and different arrangements of the tool–work-piece system. The main goal of these kinds of measurements is to determine the cutting coefficients in different directions which are essential to predict the stability of certain cutting operations (Altintas & Budak 1995; Bayly *et al.* 2003; Warminski *et al.* 2003; Merdol & Altintas 2004; Insperger & Stepan 2004; Zatarain *et al.* 2006). The last set of experimental data in Figure 2(d) was collected from a series of orthogonal cutting identification tests (see, Acknowledgement).

In the subsequent sections we will show that the inflexion of the cutting force characteristics has a central role in the nonlinear vibrations, and consequently, in the size of the unsafe or bi-stable zone.

b) Regenerative effect

Figure 1(b) presents the variation of the instantaneous chip thickness $h(t)$ as a function of the present position $q(t)$ and the delayed position $q(t-\tau)$ of the tool, given by

$$h(t) = q(t-\tau) - q(t) + h_0, \tag{5}$$

where h_0 is the prescribed chip thickness, $\tau = 2\pi/\Omega$ is the period of the rotating work-piece and Ω is its angular velocity. Since, the cubic expression (3) of the cutting force depends on the actual chip thickness (5), the equation of motion (1) has the form

$$\ddot{q}(t) + 2\kappa\,\omega_n\,\dot{q}(t) + \omega_n^2\,q(t) = \frac{w}{m}(\rho_1\,h(t) + \rho_2\,h^2(t) + \rho_3\,h^3(t)). \tag{6}$$

Its trivial solution provides the equilibrium corresponding to stationary cutting at

$$q_0 = \frac{1}{m\,\omega_n^2} F_q(h_0),$$

where the spring force is balanced by the cutting force (3). Introducing the perturbation x around this position by $x(t) = q(t) - q_0$, and rescaling time t with the angular natural frequency ω_n, and the tool position perturbation x with the theoretical chip thickness h_0 leads to the dimensionless variables and parameters

$$\tilde{t} = \omega_n\,t, \quad \tilde{x} = x/h_0,$$

$$\tilde{w} = w\frac{\rho_1 + 2\rho_2\,h_0 + 3\rho_3\,h_0^2}{m\,\omega_n^2}, \quad \tilde{\tau} = \omega_n\,\tau, \quad \tilde{\Omega} = \frac{2\pi}{\tilde{\tau}} = \frac{\Omega}{\omega_n},$$

$$\eta_2 = h_0\frac{\rho_2 + 3\rho_3\,h_0}{\rho_1 + 2\rho_2\,h_0 + 3\rho_3\,h_0^2}, \quad \eta_3 = h_0^2\frac{\rho_3}{\rho_1 + 2\rho_2\,h_0 + 3\rho_3\,h_0^2}. \tag{7}$$

In the dimensionless form of the equation of motion, the derivatives with respect to dimensionless time are denoted by primes, while all the tildes are henceforth dropped. With the vector

$$\mathbf{y} = \mathrm{col}(y_1, y_2) = \mathrm{col}(x, x'),$$

the new form of the equation of motion (6) is

$$\mathbf{y}'(t) = \mathbf{L}\,\mathbf{y}(t) + \mathbf{R}\,\mathbf{y}(t-\tau) + \mathbf{g}(\mathbf{y}(t), \mathbf{y}(t-\tau)), \tag{8}$$

where the linear part is defined by the non-delayed and delayed coefficient matrices

$$\mathbf{L} = \begin{bmatrix} 0 & 1 \\ -(1+w) & -2\kappa \end{bmatrix}, \qquad \mathbf{R} = \begin{bmatrix} 0 & 0 \\ w & 0 \end{bmatrix},$$

respectively, and the nonlinear part is given by

$$\mathbf{g}(\mathbf{y}(t), \mathbf{y}(t-\tau)) = w\begin{bmatrix} 0 \\ \eta_2\,(y_1(t-\tau) - y_1(t))^2 + \eta_3\,(y_1(t-\tau) - y_1(t))^3 \end{bmatrix}.$$
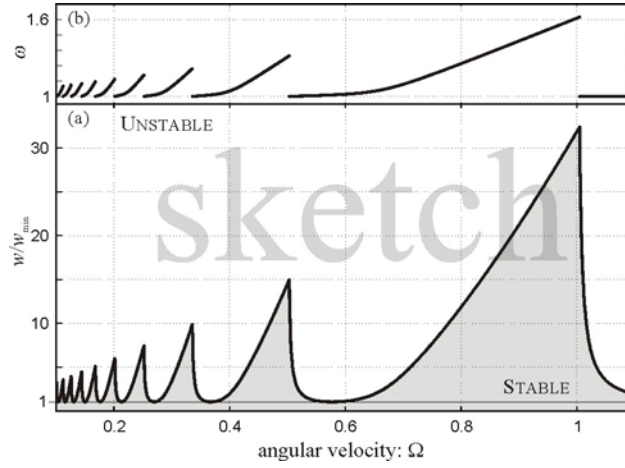
Figure 3. In panel (a) the linear stability chart can be seen in normalised, dimensionless technological parameter space ($w/w_{\min}$, Ω). In panel (b) the dimensionless frequencies ω of the self excited vibrations are presented at the limits of stability. (Here $\kappa = 0.01$.)

c) Operator formulation

From the theory of functional differential equations (Hale 1977), the phase space of the delayed systems is infinite dimensional. In order to represent the equation of motion in the infinite dimensional phase space of the continuous functions defined by the shift

$$\mathbf{y}_t(\theta) := \mathbf{y}(t+\theta), \quad \theta \in [-\tau, 0],$$

one can transform the delay-differential equation (DDE) (8) into the operator differential equation (OpDE)

$$\mathbf{y}_t' = \mathcal{A}\mathbf{y}_t + \mathcal{F}(\mathbf{y}_t), \tag{9}$$

where the linear operator $\mathcal{A}$ and the nonlinear operator $\mathcal{F}$ are defined by

$$(\mathcal{A}\mathbf{y}_t)(\theta) = \begin{cases} \mathbf{y}_t^o(\theta), & \text{if } \theta \in [-\tau, 0), \\ \mathbf{L}\,\mathbf{y}_t(0) + \mathbf{R}\,\mathbf{y}_t(-\tau), & \text{if } \theta = 0, \end{cases}$$

$$(\mathcal{F}(\mathbf{y}_t))(\theta) = \begin{cases} \mathbf{0}, & \text{if } \theta \in [-\tau, 0), \\ \mathbf{g}(\mathbf{y}_t(0), \mathbf{y}_t(-\tau)), & \text{if } \theta = 0. \end{cases}$$

The superscript circle denotes derivative with respect to the 'past time' θ, which equals the derivative with respect to the (dimensionless) time

$$\mathbf{u}_t^o(\theta) := \frac{\mathrm{d}}{\mathrm{d}\theta}\mathbf{u}_t(\theta) = \mathbf{u}'(t+\theta).$$

The OpDE formulation (9) corresponds to the DDE form (8), or to the traditional form (6) of the equation of motion and makes it possible to carry out a correct nonlinear analytical investigation via linear stability analysis, Centre Manifold reduction and Normal Form calculation.

3. Linear stability

From an engineering point of view, the linear stability charts are preferred to be represented in a plane formed by the spindle speed and chip width. In the stable domains of these charts, those parameter regions are identified where stationary cutting is possible without chatter. These regions can be determined by the stability investigation of the linear part $\mathbf{y}_t' = \mathcal{A}\,\mathbf{y}_t$ of the OpDE (9). The usual substitution of the exponential trial solution $\mathbf{y}_t(\theta) = \mathbf{s}(\theta)e^{\lambda t}$ into the linear OpDE leads to the infinite dimensional eigenvalue/eigenvector problem

$$(\mathcal{A} - \lambda\,\mathcal{I})\,\mathbf{s} = \mathbf{0}, \tag{10}$$

where $\mathcal{I}$ denotes the unit operator. This provides the characteristic function

$$D(\lambda) = \det(\lambda\,\mathbf{I} - \mathbf{L} - \mathbf{R}\,e^{-\lambda\tau}),$$

for the complex characteristic exponents λ satisfying the characteristic equation

$$\mathrm{Ker}\{\mathcal{A} - \lambda\mathcal{I}\} \neq \{\mathbf{0}\} \quad \Leftrightarrow \quad D(\lambda) = 0 \quad \Leftrightarrow \quad \lambda^2 + 2\kappa\lambda + 1 + w - we^{-\lambda\tau} = 0. \tag{11}$$

If the infinitely many complex characteristic roots λ_k ($k \in \mathbb{N}$) of the characteristic function (11) satisfy $\mathrm{Re}\,\lambda_k < 0$ for all k then the trivial solution (i.e., stationary cutting) is locally asymptotically stable; if there exists a k with $\mathrm{Re}\,\lambda_k > 0$ then it is unstable. At the linear stability boundaries, the characteristic function (11) has purely imaginary complex conjugate roots $\lambda = \pm\mathrm{i}\,\omega$, where $\omega \in \mathbb{R}^+$ is the dimensionless angular frequency of the self excited vibrations arising close to the stability limit.

By substitution of the purely imaginary characteristic roots into (11), the stability limits (so-called 'lobes') can be expressed analytically as a parametric function of the frequency ω (see, e.g., Stepan 2001):

$$w_{\text{stab}}(\omega) = \frac{(\omega^2 - 1)^2 + 4\kappa^2\omega^2}{2(\omega^2 - 1)}, \quad \tau(\omega) = \frac{2}{\omega}\left(j\pi - \arctan\frac{\omega^2 - 1}{2\kappa\omega}\right),$$

$$j \in \mathbb{N}^+ \quad \text{and} \quad \Omega(\omega) = 2\pi/\tau(\omega), \quad \omega \in (1, +\infty)\ . \tag{12}$$

The minimum value of the stability limits can be expressed in closed form by

$$w_{\min} = 2\kappa(1 + \kappa)\ .$$

The stability boundaries w_{stab} will be normalized with respect to this minimal value $w_{\min}$ in order to show stability charts independent of the small (~ 0.01) damping ratio parameter. These expressions provide the stability boundary curves (or lobes) $w_{\text{stab}}(\Omega)$ in Figure 3(a), while the (dimensionless) vibration frequency ω against the cutting speed is given above the lobes at the stability limits in Figure 3(b). Note that the frequencies of the corresponding self-excited vibrations are all larger than the natural frequency of the system, that is, $\omega > 1$. The lobe structure in Figure 3(a) is typical for delayed oscillators (see Hu & Wang 2002, Kyrychko et al. 2006).

4. Nonlinear investigation

In this section, an overview of the applied algebraic and numerical techniques is given to clarify the dynamic effects of the nonlinear cutting force characteristics. First, the lengthy *Hopf bifurcation* calculation is summarized in order to provide analytical estimate for the nonlinear vibrations in the system. Then, numerical methods are used to check the different kinds of nonlinear behaviour and also to make the results more quantitatively more accurate.

a) Hopf bifurcation calculation

The fixed point becomes non-hyperbolic at the stability limit (Figure 3(a)) with increasing (dimensionless) chip width w that will be considered as a bifurcation parameter. At its critical value $w_{\text{stab}}(\omega)$ in (11), two pure imaginary eigenvalues $\lambda_{1,2} = \pm i\omega$ exist. As the bifurcation parameter w increases through $w_{\text{stab}}(\omega)$, these characteristic roots cross the imaginary axis with nonzero (actually, positive) speed since the implicit differentiation of the characteristic equation (11) gives

$$\gamma(\omega) := \text{Re}\left(\frac{d\lambda}{dw}\bigg|_{\lambda = i\omega}\right) = 2\frac{(\omega^2 - 1)^2}{w_{\text{stab}}(\omega)} \frac{\gamma_1(\omega)}{\gamma_2(\omega)} > 0,$$

with the positive expressions

$$\gamma_1(\omega) = 4\kappa^2 \tau(\omega)\omega^2 + 4\kappa(\omega^2 + 1) + \tau(\omega)(\omega^2 - 1)^2 > 0, \qquad (13)$$

$$\gamma_2(\omega) = 16\kappa^4 \tau^2(\omega)\omega^4 + 32\kappa^3\tau(\omega)\omega^2(\omega^2 - 1) + 8\kappa\tau(\omega)(\omega^2 - 1)^2(1 + 3\omega^2) +$$

$$8\kappa^2(\omega^2 - 1)^2(2 + \tau^2(\omega)\omega^2) + (\omega^2 - 1)^2(16\omega^2 + \tau^2(\omega)(\omega^2 - 1)^2) > 0,$$

for all $\omega > 1$, $\kappa > 0$. This means that the so-called transversality condition is fulfilled (Guckenheimer & Holmes 1983), and a *Hopf bifurcation* occurs along the linear stability limits. Consequently, a periodic orbit exists in a sufficiently small region of the fixed point. The stability/instability of this periodic motion depends on the super-/subcritical sense of the *Hopf bifurcation*. The *Hopf bifurcation* calculation results in the *Poincare-Lyapunov constant* (PLC) $\Delta(\omega)$ (<0 or >0) that determines the (super- or subcritical, respectively) sense of the bifurcation. For the bifurcation parameter w close enough to its critical value $w_{\text{stab}}(\omega)$, this also leads to the estimate

$$r(\omega, w) \approx \sqrt{-\frac{\gamma(\omega)}{\Delta(\omega)}\left(w - w_{\text{stab}}(\omega)\right)} \qquad (14)$$

for the amplitude r of the corresponding approximately $(2\pi/\omega)$-periodic motion that is located in the 2-dimensional Centre Manifold embedded in the infinite dimensional phase space. At the origin, this Centre Manifold is tangent to the plane spanned by the real and the imaginary parts of the critical eigenvectors $\mathbf{s}_{1,2}$ of the operator $\mathcal{A}$ belonging to the critical eigenvalues $\lambda_{1,2} = \pm i\omega$. Thus, the periodic solution of the OpDE can be approximated as

$$\mathbf{y}_t(\theta) = \mathbf{y}(t + \theta) \approx r(\omega, w)(\cos(\omega t)\text{Re}\,\mathbf{s}_1(\theta) - \sin(\omega t)\text{Im}\,\mathbf{s}_1(\theta)), \qquad (15)$$

and consequently, the approximation of the periodic solution of the DDE (8) assumes the form

$$\mathbf{y}(t) = \mathbf{y}_t(0) = \begin{bmatrix} x(t) \\ x'(t) \end{bmatrix} \approx r(\omega, w) \left(\operatorname{Re} \mathbf{s}_1(0) \cos(\omega t) - \operatorname{Im} \mathbf{s}_1(0) \sin(\omega t) \right).$$

To determine the critical eigenvectors, it is easy to solve the boundary value problem defined by the infinite dimensional eigenvalue/eigenvector problem (10) at the borders of stability:

$$(\mathcal{A} \mp i\omega \mathcal{I}) \mathbf{s}_{1,2} = \mathbf{0} \quad \Rightarrow \quad \mathbf{s}_{1,2}(\theta) = \begin{bmatrix} \cos \omega\theta \\ -\omega \sin \omega\theta \end{bmatrix} \pm i \begin{bmatrix} \sin \omega\theta \\ \omega \cos \omega\theta \end{bmatrix}. \tag{16}$$

However, the calculation of the PLC $\Delta(\omega)$ is rather lengthy and not presented here. The calculation follows the same algebraic steps described for similar delayed oscillator examples in (Campbell & Bélair 1995; Stepan 1997; Nayfeh & Balachandran 1995; Kalmár-Nagy *et al.* 2001; Orosz & Stepan 2004) and it can be found in (Dombovari 2006, Dombovari *et al.* 2007) in detail. The result is

$$\Delta(\omega) = \frac{1}{2}(\omega^2 - 1)\gamma(\omega)\left(3\eta_3 + \frac{\delta_1(\omega)}{\delta_2(\omega)}\eta_2^2 \right), \tag{17}$$

where

$$\delta_1(\omega) = 16\kappa\,\omega^2\,(48\kappa^5\,\tau(\omega)\,\omega^4 + 48\kappa^4\,\omega^2\,(\omega^2 - 1)) + 384\kappa^4\,\tau(\omega)\,\omega^4\,(\omega^2 - 1)^2 +$$
$$48\kappa^2\,\tau(\omega)\,\omega^2\,(\omega^2 - 1)^4 + 64\kappa^3\,\omega^2\,(\omega^2 - 1)^2\,(1 + 17\,\omega^2) - 32\kappa\,\omega^2\,(\omega^2 - 1)^4\,(4\,\omega^2 - 1),$$

$$\delta_2(\omega) = \gamma_1(\omega)(\omega^2 - 1)(36\kappa^2\,\omega^2 + (\omega^2 - 1)^2\,(4\,\omega^2 - 1)^2) > 0,$$

and the always positive $\gamma_1(\omega)$, $\tau(\omega)$ and $w_{\text{stab}}(\omega)$ are given by (13) and (12) respectively. Clearly, the sign of $\Delta(\omega)$ depends on the possible negative values of $\delta_1(\omega)$. A lengthy but straightforward algebraic manipulation proves the following analytical estimate:

$$\frac{\delta_1(\omega)}{\delta_2(\omega)} > -1, \text{ for any } \omega \in (1, +\infty) \text{ and } \kappa > 0.$$

Actually, numerical investigation shows that the stricter estimate $\delta_1(\omega)/\delta_2(\omega) > -0.36$ holds as well. Also, the cutting force characteristics must always be increasing, which means for the 3 parameters $\rho_{1,2,3}$ of the cubic polynomial cutting force F_q in (3) that

$$\frac{\partial F_q}{\partial h}(h) \geq \frac{\partial F_q}{\partial h}(h_{\text{inf}}) = w\left(\rho_1 - \frac{1}{3}\frac{\rho_2^2}{\rho_3} \right) > 0, \qquad \Leftrightarrow \qquad 3\rho_1\rho_3 - \rho_2^2 > 0.$$

Using these estimates and the relations (7) between the parameters $\eta_{2,3}$ and the original $\rho_{1,2,3}$ parameters of the nonlinear cutting force, lower bounds can be given for the PLC by

$$\Delta(\omega) > \frac{1}{2}(\omega^2 - 1)\gamma(\omega)(3\eta_3 - \eta_2^2) = \frac{1}{2}\frac{h_0^2(\omega^2 - 1)\gamma(\omega)}{(\rho_1 + 2\rho_2 h_0 + 3\rho_3 h_0^2)^2}(3\rho_1\rho_3 - \rho_2^2) > 0.$$
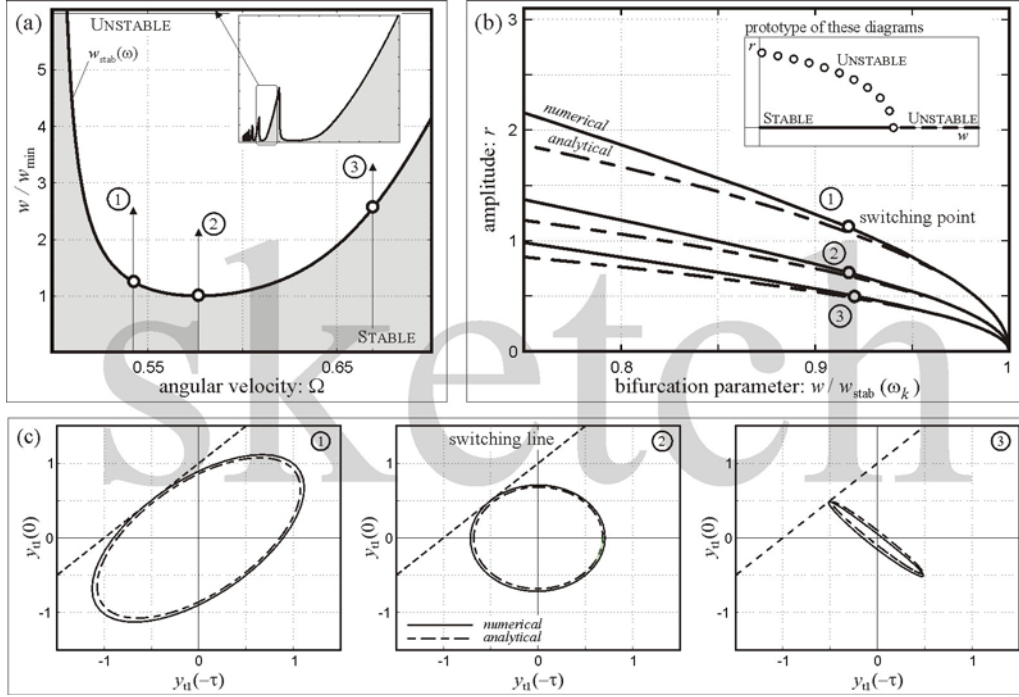
Figure 4. In panel (a) three parameter points are marked at (a lower value) ω_1=1.005, at the minimum point ω_2=1.01 and at (a higher value) ω_3=1.1 dimensionless vibration frequency of the second lobe. In panel (b) both numerically and analytically approximated bifurcation diagrams are presented which emerge from the chosen bifurcation points for ω_k, k=1,2,3. In the last panel (c) a planar projection of the unstable trajectories can be seen at the loss of contact parameters of the period-one branches where they just touch the 'switching line'. (κ =0.01, h_0 = 0.04 [mm]).

Thus, the *Hopf bifurcation* is subcritical all along the stability lobes if the gradient of the cubic cutting force function is positive at the inflexion point. A negative derivative at a possible inflexion point on the cutting force characteristic is physically unreasonable because the system would have a 'static' instability (a saddle-node bifurcation), which is rarely experienced in machine tool dynamics. As an important result of the above *Hopf bifurcation* calculation, it can be concluded that unstable oscillations exist around the locally stable stationary cutting when the chip width gets close to its critical value along the linear stability boundaries. This result is a generalization of the same conclusion of Kalmár-Nagy & Pratt 1999 and Wahi & Chatterjee 2005, which was derived for the power-law approximation of the cutting force, where hence the possibility of an inflexion point was excluded.

b)   Amplitude estimation of unstable oscillation

The approximation of the unstable periodic motion gives useful information about the kind of perturbations which allow stationary cutting. The substitution of the eigenvectors (16) into the periodic solution estimate (15) gives

$$x(t) \approx r(\omega, w) \cos(\omega t), \qquad (18)$$

while the substitution of the PLC (17) into the amplitude estimate (14) results in

$$r(\omega, w) \approx \sqrt{\frac{2}{\omega^2 - 1} \frac{\delta_2(\omega)}{\delta_1(\omega)\eta_2^2 + 3\,\delta_2(\omega)\eta_3}} \sqrt{w_{\text{stab}}(\omega) - w}. \qquad (19)$$
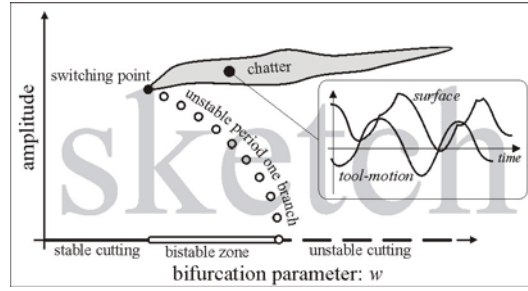
10

Figure 5 shows a realistic bifurcation diagram in case of orthogonal cutting. The 'outside' grey area represents the chattering motion when the tool leaves the surface of the work-piece at least once in every period. The sub-panel presents an estimated non-smooth nature of the surface in the chatter area.

Clearly, unstable oscillations exist for $w < w_{\text{stab}}(\omega)$, that is, when the chip width is smaller than its critical value. The corresponding dimensionless bifurcation diagrams at 3 points of the 2$^{\text{nd}}$ lobe of the stability chart are presented in Figure 4(b) by the curves denoted 'analytical'. The curves represent unstable vibration amplitudes for $w/w_{\text{stab}}(\omega) < 1$ with different curvatures for different (dimensionless) cutting speeds.

c) Path-following

The approximation of the unstable limit cycle gets worse as the chip thickness parameter gets far below its critical value at the stability limit. Moreover, below a certain limit, the unstable periodic orbit does not exist at all since the vibration amplitudes become so large that the tool actually loses contact with the work-piece. In order to check the range of validity (and also the correctness) of the analytical treatment, the continuation software DDE-BIFTOOL (Engelborghs *et al.* 2002) was applied to follow the closed unstable orbits in the parameter space. This software uses the collocation method to solve the boundary value problem of the returned closed orbits of a delayed system.

The corresponding unstable periodic orbits are represented by their amplitude curves denoted 'numerical' in the dimensionless bifurcation diagram of Figure 4(b). The results of the path-following method show very good quantitative agreement with the analytical results of the *Hopf bifurcation* calculation in the region $0.9 < w/w_{\text{stab}}(\omega) \leq 1$.

5. The region of bi-stability

As explained above, the identified unstable periodic motion exists only for that parameter region of the chip thickness where the tool does not leave the work-piece. This region is called '*bi-stable*' or the *unsafe zone* because the vibrations will settle to the locally stable stationary cutting 'inside' the unstable orbit only, while 'outside' the unstable orbit the vibrations will grow until the motion settles to a large-amplitude complex oscillation that involves repeated loss of contact between the tool and the work-piece (see Figure 5).

In order to find the boundaries of the unsafe zone where the unstable periodic orbits exist, one can consider the projection of the infinite dimensional phase space, that is, the projection to the plane $(y_{t1}(-\tau), y_{t1}(0))$, or equivalently, to the plane $(x(t - \tau), x(t))$ of the delayed and the actual dimensionless perturbations. These projections of the unstable orbits (both their analytical and numerical approximations) are presented in panel (c) of Figure 4 for chip width parameters $w_{\text{loss}}(\omega)$ where they just touch the so-called 'switching line' $y_{t1}(0) = 1 + y_{t1}(-\tau)$ that represents the first loss of contact between the tool and the work-piece.
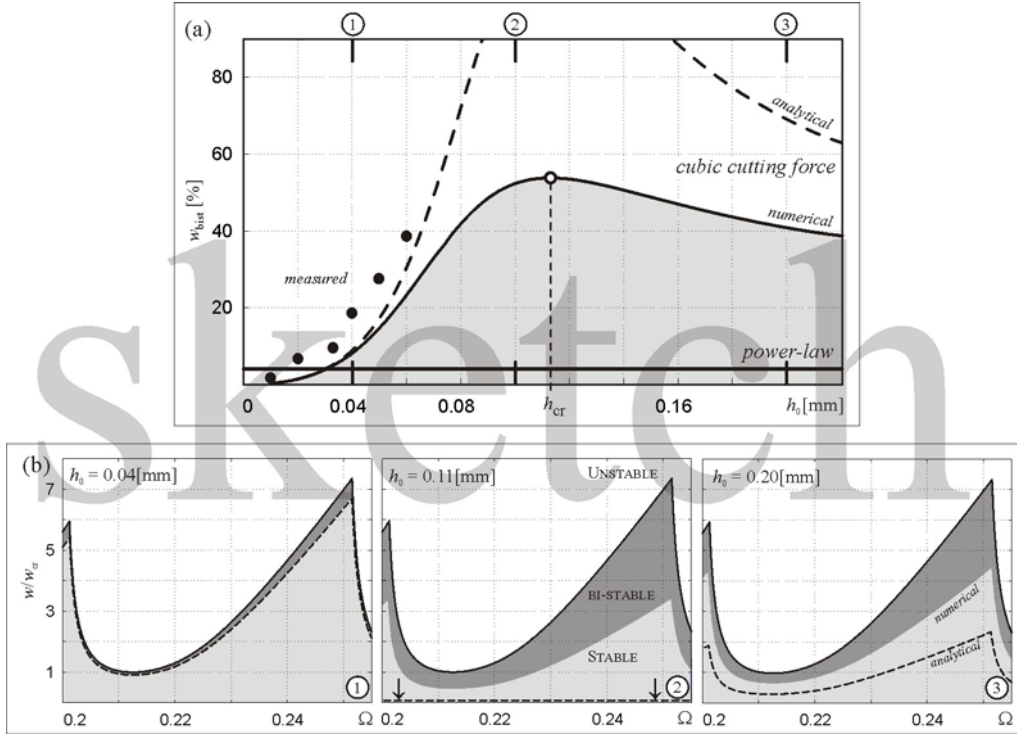
Figure 6. In panel (a) the relative widening of the bi-stable region is presented for cubic and power-law cutting force characteristics. (dashed: analytical solution, continuous: computed by DDE-BIFTOOL, dots: results of *Tobias'* measurements (Shi & Tobias 1984)). In panel (b) three intersections are shown with respect to the desired chip thickness h_0 of the 4th lobe and its unsafe zone (grey area). Here $\kappa = 0.01$.

The definition (5) of the actual chip thickness provides a simple algebraic formulation for the condition of the loss of contact in the form

$$h(t)/h_0 = 0 \quad \Rightarrow \quad x(t) - x(t-\tau) = 1, \quad \text{for some } t > 0, \tag{20}$$

which determines the 'switching line' of slope 1 shifted by 1 in Figure 4(c). Substituting the analytical estimate (18) of the critical unstable periodic motion into (20) at the critical chip width parameter $w_{\text{loss}}(\omega)$ and using formulae (12) for the linear stability limit yields

$$x(t) - x(t-\tau) \approx r(\omega, w_{\text{loss}}(\omega)) \left(\cos(\omega t) - \cos(\omega t - \tau(\omega)) \right) =$$
$$r(\omega, w_{\text{loss}}(\omega)) \sqrt{\sin^2(\tau(\omega)) + (1 - \cos(\tau(\omega))^2} \cos(\omega t + \psi) =$$
$$\frac{r(\omega, w_{\text{loss}}(\omega))}{w_{\text{stab}}(\omega)} \sqrt{(\omega^2 - 1)^2 + 4\kappa^2 \omega^2} \cos(\omega t + \psi).$$

With the help of the amplitude estimate (19), the loss of contact condition (20) can be reformulated in terms of the chip thickness parameter w_{loss} as a function of the frequency parameter ω used to parameterize the stability lobes:

$$w_{\text{loss}}(\omega) = w_{\text{stab}}(\omega) \left(1 - \frac{1}{2} \frac{\delta_1(\omega)\eta_2^2 + 3\delta_2(\omega)\eta_3}{\delta_2(\omega)} \right).$$

These values of the chip width are also depicted in Figure 4(b) marked with tiny circles and by the text 'switching point' for the 3 different cases of cutting speeds. These values, which characterize the loss of contact parameters, are in the range of 0.9 – 0.92. This range is in agreement with the

range measured experimentally by Shi & Tobias 1984. This means that the bi-stable or unsafe zone is within the range

$$w_{\text{loss}}(\omega) < w < w_{\text{stab}}(\omega) \ ,$$

and the curves representing the unstable orbits in Figure 4(b) are extended hypothetically to the left of the switching points at $w_{\text{loss}}(\omega)$, since they do not exist for $w < w_{\text{loss}}(\omega)$.

Finally, the bi-stable regions can also be represented in the stability charts. The shaded regions below the stability lobes in Figure 6(b) can be determined easily with the help of the ratio of the width of the bi-stable region relative to the critical chip width parameter at the linear stability limit:

$$w_{\text{bist}}(\omega) = \frac{w(\omega) - w_{\text{loss}}(\omega)}{w(\omega)} = \frac{1}{4} \frac{\delta_1(\omega)\eta_2^2 + 3\delta_2(\omega)\eta_3}{\delta_2(\omega)} \ . \tag{21}$$

Note that the parameters $\eta_{2,3}$ of the nonlinear cutting force characteristics depend strongly on the theoretical chip thickness h_0 as indicated by formulae (7). Consequently, the size of the bi-stable region also depends on h_0 as it can be observed also in Figure 6. In case of the power-law approximation, the width of this bi-stable region does not vary at all.

Figure 6(b) shows the size of the bi-stable region in % according to formula (21) as a function of the chip thickness h_0 where the nonlinear cutting force parameters $\rho_{1,2,3}$ are fixed at the values of Figure 2(b) taken from (Shi & Tobias 1984). The experimental results from (Shi & Tobias 1984) are denoted by dots and they match the analytical prediction closely. This is remarkable since the conventional power-law characteristics provide a constant ~ 4 % width for the bi-stable region. The most critical theoretical chip thickness h_{cr}, where the size of the bi-stable region is maximal, can be calculated analytically by

$$h_{\text{cr}} = -\frac{\rho_1}{\rho_2} \ .$$

In the meantime, the quantitatively more accurate path-following method determined the switching points more precisely, and the real size of the maximal bi-stable zone is shown to be about half the size of the analytical estimation (see Figure 6). This value is nevertheless at about 50 %, which is circa 12 times larger than the one predicted by the power-law formulation.

6. Conclusions

Stationary cutting force measurements indicate that the nonlinear cutting force characteristics often involve an inflexion point in the otherwise monotonous increasing function of chip thickness. The conventional power-law approximation of the empirical cutting force is not able to describe this inflexion point. We have analysed the effect of this inflexion point from the nonlinear dynamics viewpoint when a cubic polynomial approximation of the cutting force characteristics is used.

The conventional power-law approximation has several advantages from the viewpoint of the optimal design of the parameters of the technology, but it has serious disadvantages from the viewpoint of predicting machine tool chatter. On the one hand, the application of the power-law in a Newtonian equation of machine tool vibration violates the uniqueness of the solution in forward time and also causes unpredictable errors during the numerical simulation of large amplitude oscillations between the tool and work-piece. On the other hand, the missing inflexion point results in the prediction of a uniform and thin bi-stable region along the stability limits that does not depend on the mean (or theoretical) chip thickness. This bi-stable region jeopardises the chatter-free

cutting even for stable stationary cutting processes designed and optimized by linear theory; and the power-law approximation of the cutting force heavily underestimates the real size of this zone.

With the help of realistic cubic polynomial approximations of the nonlinear cutting force, we have proved the uniform subcriticality of the *Hopf bifurcations* along all the linear stability limits of regenerative cutting processes. The only mathematical prerequisite for this subcriticality is the natural positive slope of the cutting force characteristics at the inflexion point.

Furthermore we have estimated the width of the bi-stable region analytically. It was shown that its size varies along the stability limits and this bi-stable region could be much larger than expected before. While the linear stability boundaries increase slightly for increasing values of the theoretical chip thickness, for both power-law and cubic polynomial cutting forces, the size of the bi-stable region increases for much (actually, about 12 times) larger values in case of the presence of an inflexion point in the cutting force characteristics than the size of the bi-stable region predicted by the power-law approximations of the cutting force. The analytical results were checked by continuation software, and the above conclusions were confirmed by existing experimental results of the specialist literature (Shi & Tobias 1984) that were re-visited and re-examined from the nonlinear dynamics points of view.

References

Altintas, Y. 2000 *Manufacturing automation: metal cutting mechanics, machine tool vibrations and CNC design.* Cambridge: Cambridge University Press,.

Altintas, Y. and Budak, E. 1995 Analytical Prediction of Stability Lobes in Milling. *CIRP Annals – Manufacturing Technology*, Vol. 44, Issue 1, **pp**. 357-362.

Bayly, P. V., Halley J. E., Mann B. P. and Davies M. A. 2003 Stability of Interrupted Cutting by Temporal Finite Element Analysis. *Journal of Manufacturing Science and Engineering*, Vol. 125, Isuue 2, **pp**. 220-225.

Campbell, S. A. and Bélair, J. 1995 Analytical and symbolically-assisted investigation of Hopf bifurcations in delay-differential equations. *Can. Appl. Math. Quart.*, 3(2), **pp**. 137–154.

Campbell, S. A. and Stone, E. 2004 Stability and bifurcation analysis of a nonlinear DDE model for drilling. *Journal of Nonlinear Science* **14**, 27-57.

Davies M. A. and Burns, T. J. 2001 Thermomechanical oscillations in material flow during high-speed machining. *Phil. Trans. R. Soc. Lond. A* **359**, 821-846.

Dombovari, Z. 2006 Bifurcation analysis of a cutting process, *MSc Thesis*, University of Bristol (UK) and Budapest University of Technology and Economics (Hungary).

Dombovari, Z., Wilson, R. E. and Stepan, G. 2007 Large amplitude nonlinear vibrations in turning processes, *6th International Conference of High Speed Machining* San Sebastián, Spain.

Endres, W.J. and Loo, M. 2002 Modeling cutting process nonlinearity for stability analysis - application to tooling selection for valve-seat machining, *5th CIRP Workshop*, West Lafayette, USA.

Engelborghs, K., Luzyanina, T. and Roose, D. 2002 Numerical bifurcation analysis of delay differential equations using DDE BIFTOOL, *ACM Trans. on Math. Software* **28**, 1–21.

Guckenheimer, J. and Holmes, P. 1983 Nonlinear Oscillations, *Springer*, New York.

Hale, J. K. 1977 *Theory of functional differential equations*, New York, NY : Springer.

Insperger, T. and Stepan, G. 2004 Vibration frequencies in high-speed milling processes or a positive answer to Davies, Pratt, Dutterer and Burns. *Journal of Manufacturing Science and Engineering* **126** 481-487.

Hu, H. Y. and Wang, Z. H. 2002 *Dynamics of controlled mechanical systems with delayed feedback.* Berlin, Germany: Springer.

Kalmar-Nagy T. and Pratt R.J. 1999 Experimental and analytical investigation of the subcritical instability in metal cutting, *17th ASME Biennial Conference on Mechanical Vibration and Noise*, Las Vegas, Nevada.

Kalmár-Nagy, T., Stepan, G. and Moon, F. C. 2001 Subcritical Hopf bifurcation in the delay equation model for machine tool vibrations, *Nonlinear Dynamics* **26**, 121-142.

Kienzle, O. 1957 Spezifische schnittkräfte bei der metallbearbeitung, *Werkstattstechnik und Maschinenbau* **47**.

Kyrychko, Y.N., Blyuss K. B., Gonzalez-Buelga A., Hogan S. J. and Wagg D.J. 2006 Real-time dynamic substructuring in a coupled oscillator–pendulum system, *Proc. R. Soc. A* **462** 1271-1294.

Merdol, S.D. and Altintas, Y. 2004 Multi Frequency Solution of Chatter Stability for Low Immersion Milling, *Journal of Manufacturing Science and Engineering*, Vol. 126, Issue 3, **pp**. 459-466.

Nayfeh, A. H. and Balachandran, B. 1995 *Applied nonlinear dynamics*, New York, NY : Wiley,.

Nayfeh, A., Chin C. and Pratt, J. 1997, Applications of perturbation methods to tool chatter dynamics, dynamics and chaos in manufacturing processes, F. C. Moon (ed.), *Wiley*, New York, **pp**. 193–213.

Orosz G. and Stepan G. 2004 Hopf bifurcation calculations in delayed systems with translational symmetry, *Journal of Nonlinear Science* 14(6), 505-528, (2004).

Shi, H. M. and Tobias, S. A. 1984 Theory of finite amplitude machine tool instability, *Int. J. of Machine Tool Design and Research*, 24, **pp**. 45-69.

Stepan, G. and Kalmár-Nagy, T. 1997 Nonlinear regenerative machine tool vibrations, *ASME Design Engineering Technical Conferences*, 1997, Sacramento, California.

Stepan, G. 1989 *Retarded Dynamical Systems*, London, UK: Longman.

Stepan, G. 2001 Modelling nonlinear regenerative effects in metal cutting, *Phil. Trans. R. Soc. Lond. A* (2001) 359, **pp**. 739-757.

Stone, E., Ahmed, S., Askari, A. and Tot, H. 2005 Investigations of process damping forces in metal cutting, *Journal of Computational Methods in Science and Engineering*,.27.

Szalai, R., Stepan, G. and Hogan, S.J. 2004 Global dynamics of low immersion high-speed milling, *CHAOS* Vol. 14, No4, **pp**. 1069-1077.

Taylor, F. W. 1907 On the art of cutting metals, *Transactions of the American Society of Mechanical Engineers*, 28, 1907, 31–350.

Tlusty, J. and Spacek, L. 1954 *Self-excited vibrations on machine tools* (in Czech). Prague: Nakl CSAV..

Tobias, S. A. 1965 *Machine tool vibrations*, London, UK : Blackie.

Wahi, P. and Chatterjee, A. 2005 Regenerative tool chatter near a codimension 2 Hopf point using multiple scales, *Nonlinear Dynamics* 40: 323-338.

Warminski, J., Cartmell, M.P., Khanin, R., Wiercigroch, M. and Litak, G. 2003 Approximate analytical solutions to primary chatter in nonlinear metal cutting model, *Journal of Sound and Vibration* **259**, 917-933.

Zatarain, M., Muñoa, J., Peigné, G. and Insperger, T. 2006 Analysis of the Influence of Mill Helix Angle on Chatter Stability, *CIRP Annals - Manufacturing Technology*, Vol. 55, Issue 1, **pp**. 365-368.

Figure captions

Figure 1. Panel (a) shows the arrangement of the machine tool–work-piece system in orthogonal cutting. Panel (b) illustrates a planar mechanical model.

Figure 2. Panel (a) illustrates the power and the cubic forms of the empirical nonlinear cutting force characteristics. Panel (b) shows the result of *Tobias'* classical measurements (Shi & Tobias 1984) in the case of full immersion milling with a face mill with an even number of teeth. Panel (c) shows the fitted cubic cutting force characteristics measured by *Endres* in case of turning (Endres & Loo 2002). Panel (d) shows static cutting force measurements made using orthogonal cutting conditions (see, Acknowledgement).

Figure 3. In panel (a) the linear stability chart can be seen in normalised, dimensionless technological parameter space (w/w_{min}, Ω). In panel (b) the dimensionless frequencies ω of the self excited vibrations are presented at the limits of stability. (Here $\kappa = 0.01$.)

Figure 4. In panel (a) three parameter points are marked at (a lower value) ω_1=1.005, at the minimum point ω_2=1.01 and at (a higher value) ω_3=1.1 dimensionless vibration frequency of the second lobe. In panel (b) both numerically and analytically approximated bifurcation diagrams are presented which emerge from the chosen bifurcation points for ω_k, k=1,2,3. In the last panel (c) a planar projection of the unstable trajectories can be seen at the loss of contact parameters of the period-one branches where they just touch the 'switching line'. (κ =0.01, h_0 = 0.04 [mm]).

Figure 5 shows a realistic bifurcation diagram in case of orthogonal cutting. The 'outside' grey area represents the chattering motion when the tool leaves the surface of the work-piece at least once in every period. The sub-panel presents an estimated non-smooth nature of the surface in the chatter area.Figure 6. In panel (a) the relative widening of the bi-stable region is presented for cubic and power-law cutting force characteristics. (dashed: analytical solution, continuous: computed by DDE-BIFTOOL, dots: results of *Tobias'* measurements (Shi & Tobias 1984)). In panel (b) three intersections are shown with respect to the desired chip thickness h_0 of the 4th lobe and its unsafe zone (grey area). Here $\kappa = 0.01$.

Estimates of the bi-stable region in metal cutting